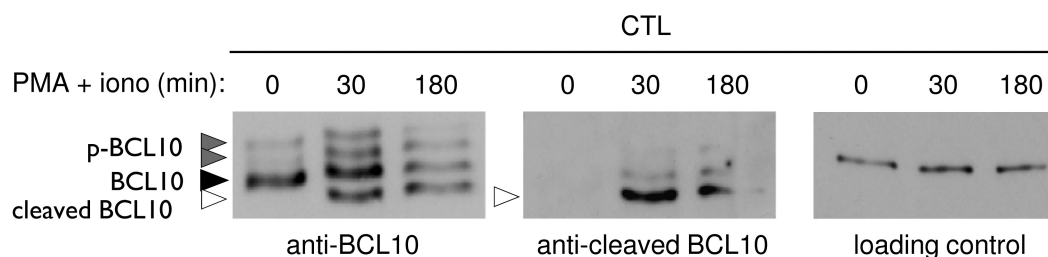


Supporting Information

Hailfinger et al. 10.1073/pnas.0907511106

A



B

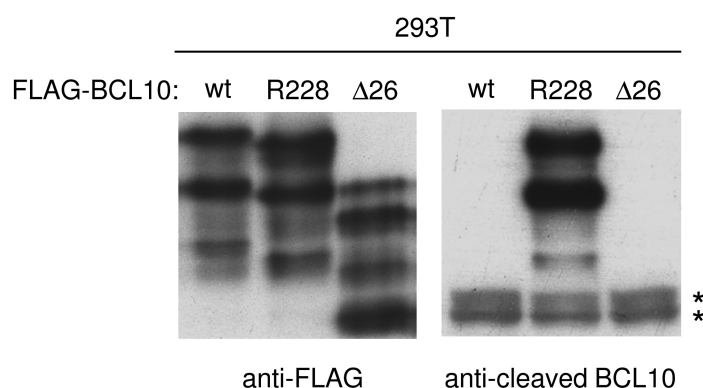


Fig. S1. Specificity of the anti-cleaved BCL10 antibody. (A) Purified human cytotoxic T-lymphocytes were stimulated as indicated, and postnuclear lysates analyzed by high resolution SDS/PAGE and Western blotting. Protein lysates (10 and 70 μ g) were analyzed using anti-BCL10 and affinity-purified anti-cleaved BCL10, respectively. The anti-cleaved BCL10 antibody specifically recognizes cleaved BCL10 (and slower migrating phosphorylated forms of cleaved BCL10), present exclusively in the stimulated cells. (B) 293T cells were transfected with expression constructs for wild-type BCL10, a BCL10 construct corresponding to cleaved BCL10 that lacks the 5 C-terminal amino acids following R228 (R228), or a BCL10 construct lacking the 26 C-terminal amino acids (Δ 26), and lysates were analyzed by Western blot using the indicated primary antibodies. In 293T cells, the anti-cleaved BCL10 also detects non-specific cross-reactive bands (*).

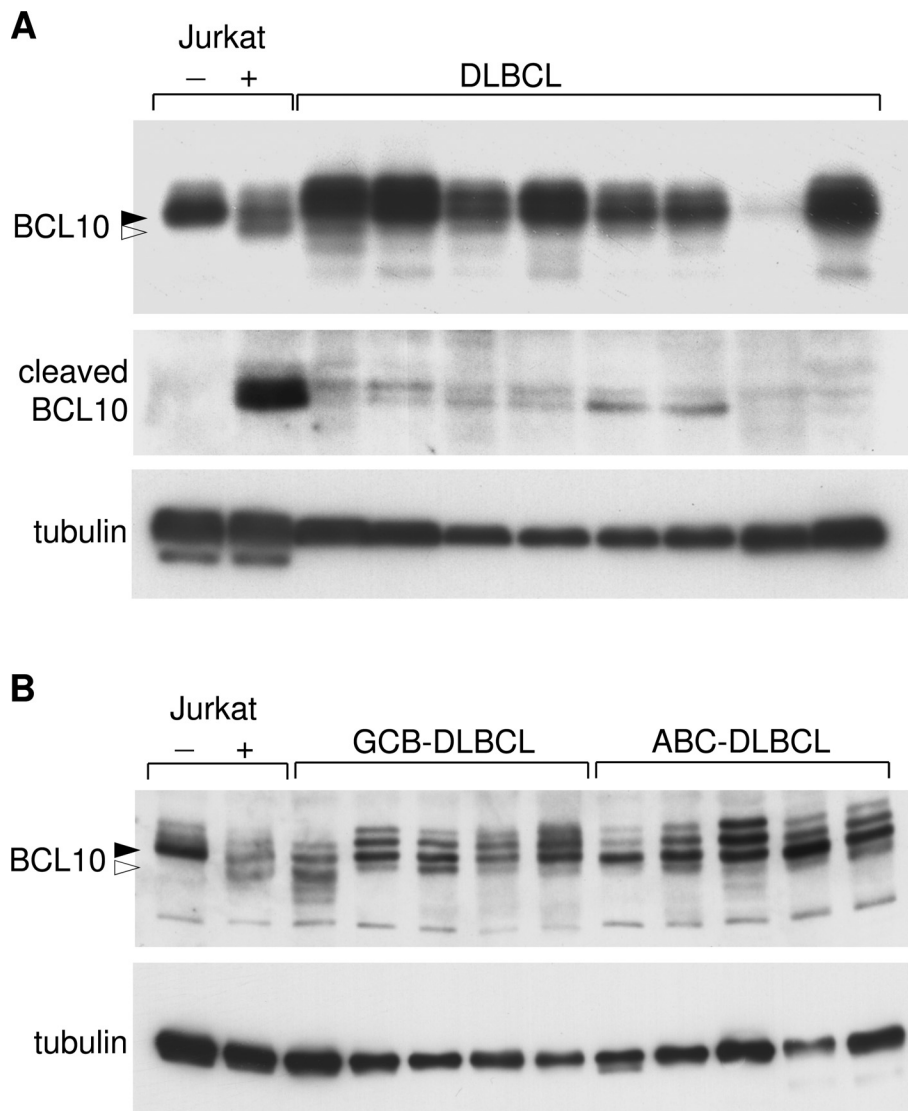


Fig. S2. BCL10 isoforms present in human diffuse large B-cell lymphomas. (A) Lysates of eight samples of frozen biopsies of patients diagnosed with DLBCL were analyzed by Western blotting using the indicated antibodies. Protein lysates (10 and 100 μ g) were analyzed using anti-BCL10 and affinity-purified anti-cleaved BCL10, respectively. Samples were derived from DLBCL at primary diagnosis that had not evolved from a low grade NHL, were negative for t (14, 18), t (11, 14), and t (8, 14), did not correspond to anaplastic DLBCL nor to primary mediastinal DLBCL. Lysates of Jurkat cells that were incubated for 30 min in the presence or absence of PMA and ionomycin were used as positive and negative controls, respectively, for the detection of cleaved BCL10. The upper and lower band detected with the antibody specific for cleaved BCL10 most likely correspond to phosphorylated and non phosphorylated isoforms of cleaved BCL10. (B) BCL10 isoforms present in human diffuse large B-cell lymphomas of the ABC and GCB subtype. Lysates of samples of frozen biopsies of patients diagnosed with DLBCL were analyzed by Western blotting using the indicated antibodies. Samples were derived from DLBCL that were classified as DLBCL of the ABC or GCB subtype by gene array. Lysates of Jurkat cells that were incubated for 30 min in the presence or absence of PMA and ionomycin were used as positive and negative controls, respectively, for the detection of cleaved BCL10. The total protein yield from these biopsies was not sufficient for detection of cleaved BCL10 using anti-cleaved BCL10 antibody.

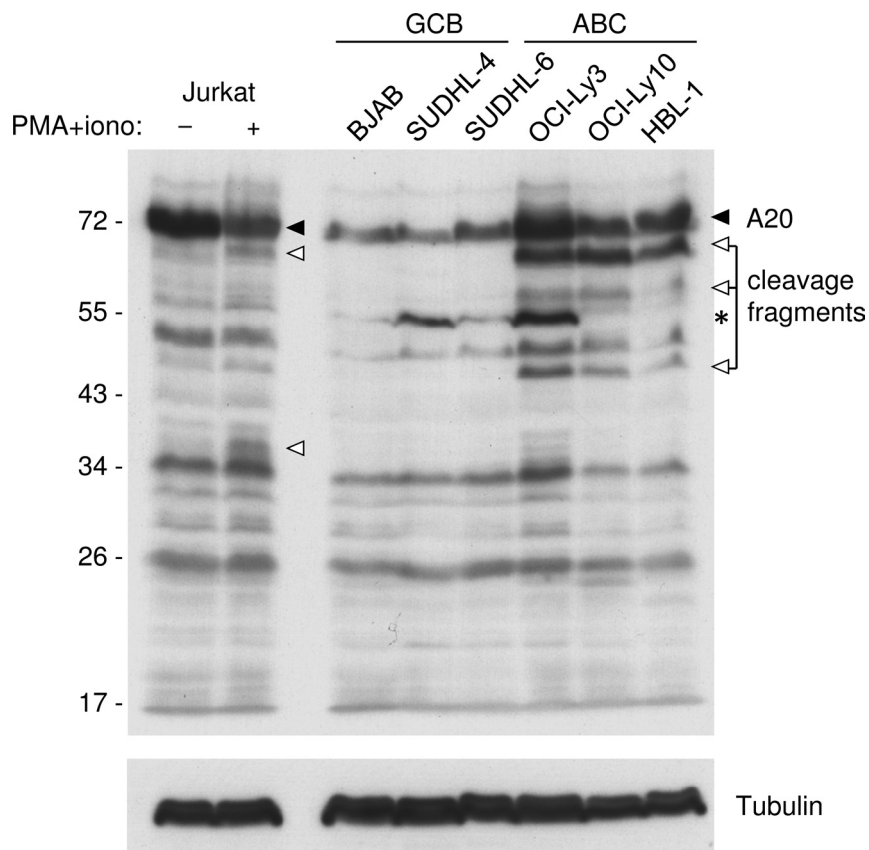


Fig. S3. Analysis of A20 in DLBCL-derived cell lines. Cell lines representative of GCB DLBCL (BJAB, SUDHL-4, and SUDHL-6) and ABC DLBCL (OCI-Ly3, OCI-Ly10, and HBL-1) were lysed and expression of A20 was assessed by Western blot (*Upper*). Loading of equal protein content was verified by blotting for tubulin (*Lower*). ABC DLBCL show strong expression of A20 that is constitutively cleaved into fragments of approximately 65, 58, and 47 kDa. Lysates of Jurkat cells, pretreated with the proteasome inhibitor MG132 for 30 min and then treated for 30 min with (+) or without (-) PMA and ionomycin, were used as a positive control for A20 cleavage. Lysates of stimulated Jurkat cells contain a fragment of 37 kDa that most likely corresponds to a previously described A20 fragment of 37 kDa (1), in addition to a fragment of 65 kDa that corresponds in size to a fragment that is present in ABC DLBCL. The asterisk (*) indicates a non specific band that was not reproducibly detected.

1. Coornaert B, et al. (2008) T cell antigen receptor stimulation induces MALT1 paracaspase-mediated cleavage of the NF-kappaB inhibitor A20. *Nat Immunol* 9:263–271.

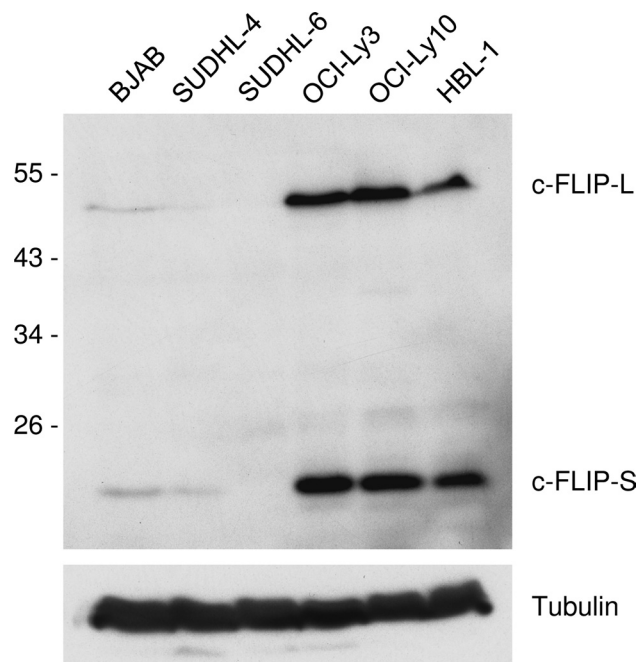
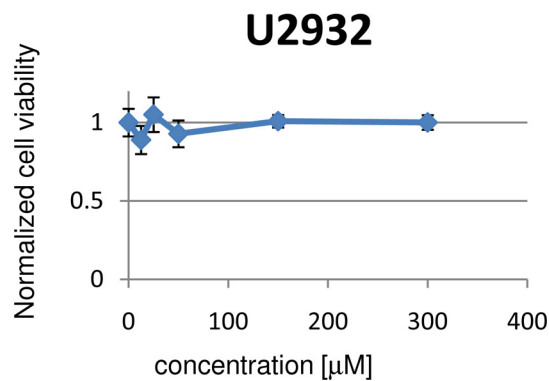
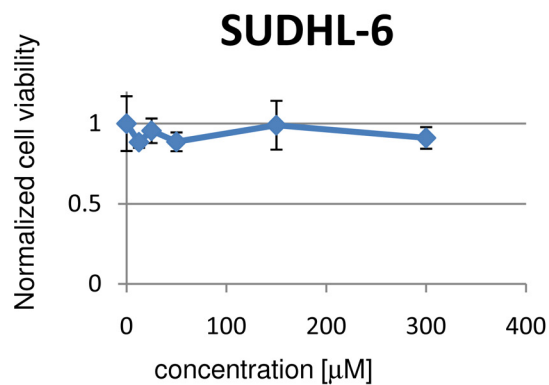
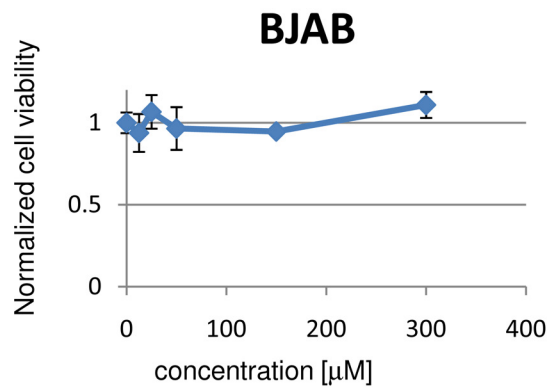


Fig. S4. Expression of c-FLIP in DLBCL-derived cell lines. Cell lines representative of ABC DLBCL (OCI-Ly3, OCI-Ly10, and HBL-1) and GCB DLBCL (BJAB, SUDHL-4, and SUDHL-6) were lysed and expression of the long and short splice isoforms of FLIP (c-FLIP-L and c-FLIP-S, respectively) was assessed by anti-c-FLIP Western blot (*Upper*). Loading of equal protein content was verified by blotting for tubulin (*Lower*).

GCB DLBCL cell lines:



ABC DLBCL cell lines:

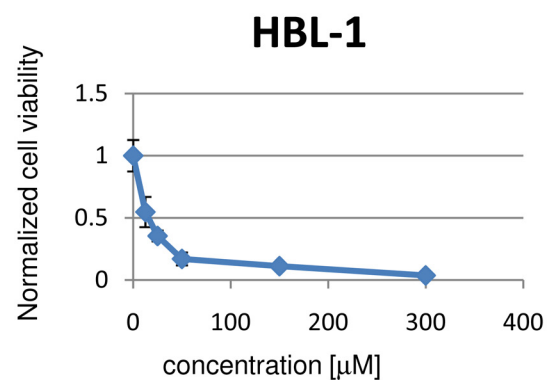
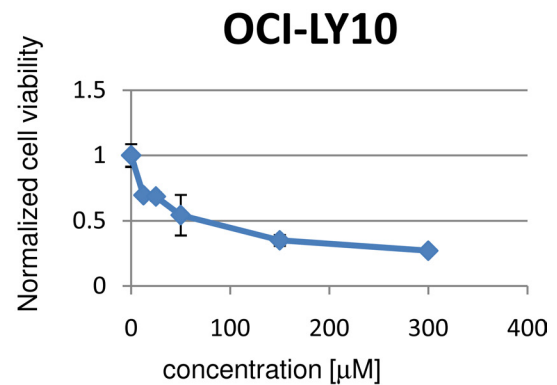
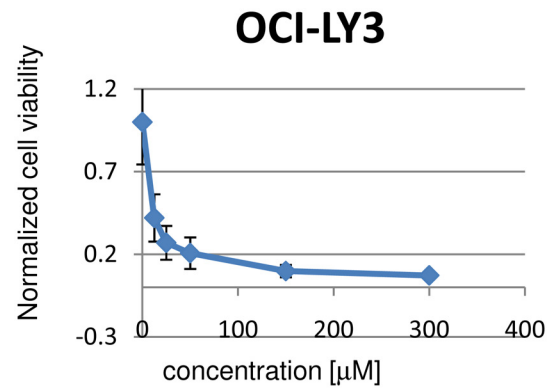


Fig. S5. Concentration dependence of apoptosis induction by the MALT1 inhibitor z-VRPR-fmk. ABC and GCB DLBCL cell lines were treated with the indicated concentration of z-VRPR-fmk at time 0 and after 24 h, and 6 days later, cell viability was assessed using the MTS/PMS assay and normalized to cells treated with solvent alone. Data represent mean values \pm standard deviation of two independent experiments performed in duplicate.

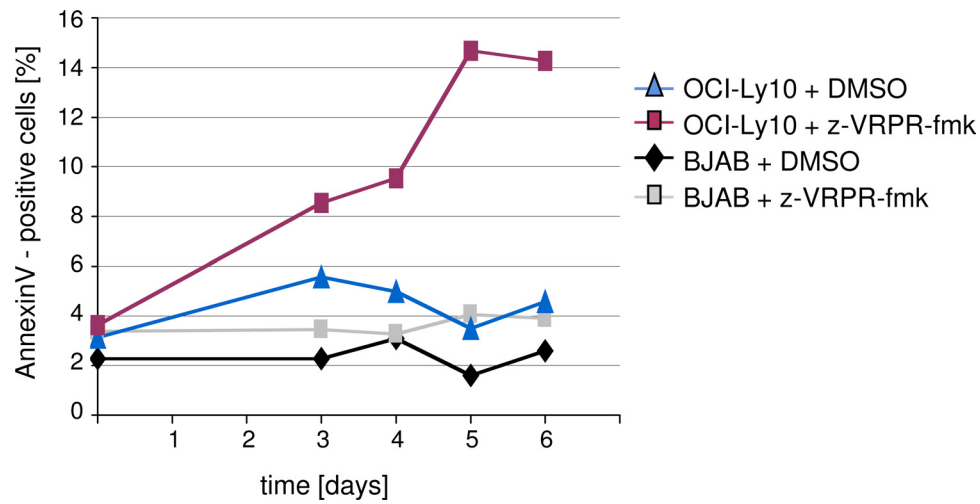


Fig. S6. Time course of apoptosis induction in OCI-Ly3 versus BJAB cells. Cell lines representative of ABC DLBCL (OCI-Ly10) and GCB DLBCL (BJAB) were treated with z-VRPR-fmk or solvent alone (DMSO) for the indicated times, and the percentage of AnnexinV-positive apoptotic cells was determined by flow cytometry.

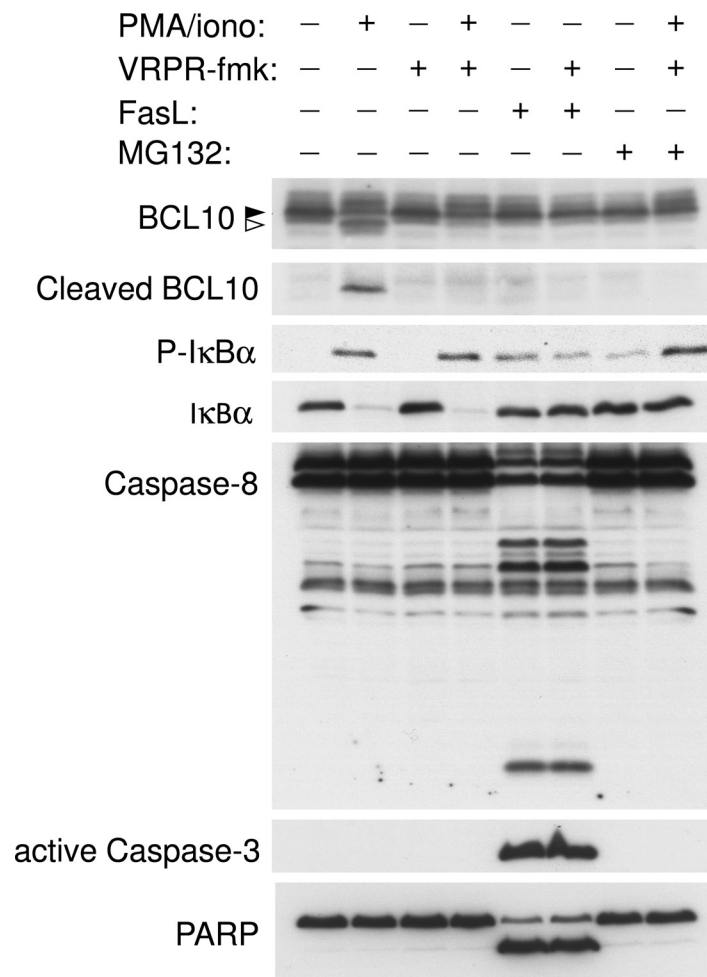


Fig. S7. Specificity of the effect of z-VRPR-fmk. Jurkat T cells were preincubated for 30 min with 50 μ M of the MALT1 inhibitor z-VRPR-fmk, 5 μ M of the proteasome inhibitor MG 132 or solvent (DMSO) alone, and stimulated using PMA and ionomycin for 30 min or recombinant active FasL for 45 min, as indicated. Postnuclear protein lysates were analyzed by Western blot using the indicated antibodies. The MALT1 inhibitor z-VRPR-fmk efficiently blocked PMA- and ionomycin-induced BCL10 cleavage by MALT1, but did not affect autoprocessing of Caspase-8, Caspase-8-dependent activation of Caspase-3 or Caspase-3-dependent cleavage of PARP. Proteasomal degradation of IκBα was efficiently blocked by MG 132, but not affected by z-VRPR-fmk.

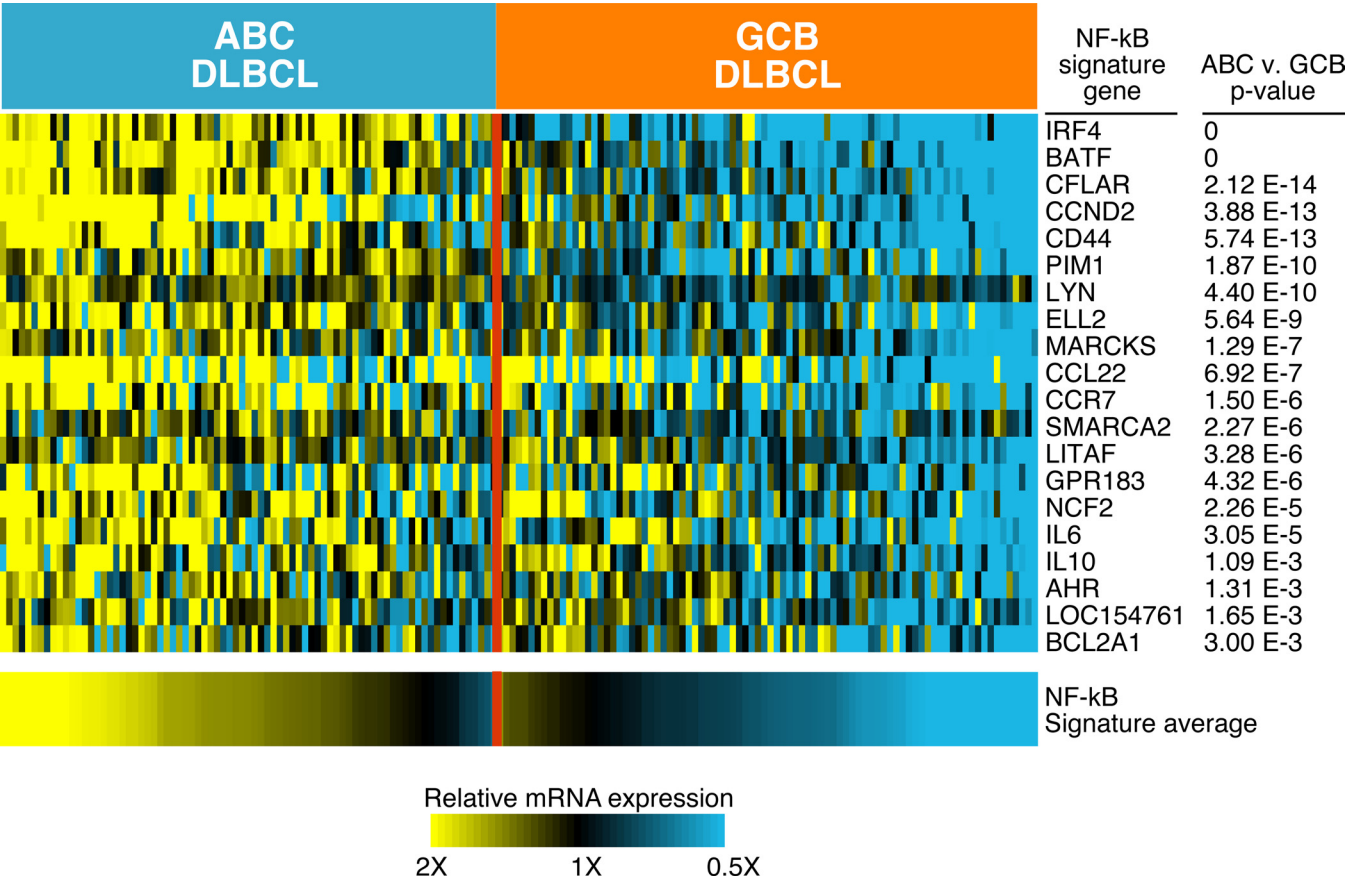


Fig. S8. Expression of NF-κB signature genes in ABC DLBCL tumor biopsies. Shown are mRNA expression levels for genes in an NF-κB target gene signature [NFκB_allLOCILy3.Ly10 signature (<http://lymphochip.nih.gov/cgi-bin/signaturedb/signatureDB.DisplayGenes.cgi?signatureID=83>) from (1–3)] that were more highly expressed in ABC DLBCL biopsy samples than GCB DLBCL biopsy samples ($P < 0.005$; fold change $>0.5 \log_2$). Each column represents Affymetrix U133plus gene expression profiling measurements from a different patient with DLBCL treated with CHOP chemotherapy (4), depicted according to the color scale shown at bottom.

1. Lam LT, et al. (2008) Cooperative signaling through the signal transducer and activator of transcription 3 and nuclear factor-(kappa)B pathways in subtypes of diffuse large B-cell lymphoma. *Blood* 111:3701–3713.

2. Lam LT, et al. (2005) Small molecule inhibitors of IkappaB kinase are selectively toxic for subgroups of diffuse large B-cell lymphoma defined by gene expression profiling. *Clin Cancer Res* 11:28–40.

3. Shaffer AL, et al. (2006) A library of gene expression signatures to illuminate normal and pathological lymphoid biology. *Immunol Rev* 210:67–85.

4. Lenz G, et al. (2008) Stromal gene signatures in large-B-cell lymphomas. *N Engl J Med* 359:2313–2323.